

# Longitudinal Analysis of Semiconductor Lasers with Low Reflectivity Facets

ROEL BAETS, JEAN-PIERRE VAN DE CAPELLE, AND P. E. LAGASSE

**Abstract**—An analysis is made of longitudinal effects in semiconductor lasers with low facet reflectivities. For this purpose, a self-consistent model is used based on the beam propagation method, which takes into account both the lateral and longitudinal dimension. The calculations show that longitudinal effects have a significant influence on the output fields in the laser.

## I. INTRODUCTION

THE numerical modeling of semiconductor laser diodes has been a subject of wide interest over the last few years. One has attempted to use these models to understand experimentally observed phenomena and also to study the parameter dependence of the diode behavior so as to apply the model in the design of new laser types.

A complete laser model, which takes into account the three-dimensional geometry, all physical dependencies and also the evolution with time, would be of enormous complexity. Therefore all authors have made use of a number of assumptions and simplifications, the choice of which is suggested by the particular aspects to be studied, or by the limitations of the calculation method. Due to this, a large number of quite different methods has been reported, an overview of which can be found in [1].

Many methods deal with the static analysis of the laser properties, such as its power-versus-current characteristics and its near and far field. In these models [2]–[4], the transversal  $x$ -dimension (perpendicular to the active layer) is mostly eliminated by applying the effective index method [5], [6] and the longitudinal  $z$ -dimension is not taken into account. Then a self-consistent calculation is done for the electron density, the gain and the power density along the lateral  $y$ -dimension. In this way such effects as gain guiding and lateral hole burning can be analyzed. Single lateral mode as well as multimode operation can be taken into consideration but abstraction is mostly made of the longitudinal modes. For the current injection various approaches are used, going from a simple imposed form for the current density [7] to a full two-dimensional solution of the semiconductor equations [8].

In this paper, we focus our attention on the longitudinal effects in the laser cavity. It is commonly assumed that longitudinal effects are of minor importance in a laser cavity, but

verification of this is generally not done. In these models, the facet reflectivities are taken into account as a distributed loss term. However, some longitudinal variation of the power density is always present, due to the power drop at the laser facets. This longitudinal power variation, which is of the order of 17 percent for facets with a power reflectivity of 32 percent, also imposes a  $z$ -dependence on the electron density (and thus on the gain and refractive index) by the effect of stimulated recombination. It is evident that these variations will increase with decreasing facet reflectivities and with increasing current beyond threshold (because of the increasing impact of field power on electron density). Apart from these longitudinal effects, which are present in every semiconductor laser, there are a number of specific cases where a longitudinal analysis may be of interest. These include, among others, those laser types in which a longitudinal geometry variation, such as a bend or a junction, is built. Such configurations have been reported in literature [9], [10]. Finally, it is well known that a number of lasers, in which a longitudinal geometry variation was not foreseen purposely, show a strongly different output beam from both facets.

Most longitudinal models do not include the lateral dimension. In [11] the efficiency of GaAlAs lasers is analyzed at high power levels, where a saturation of the gain becomes important near the facets. In [12], a simple longitudinal method was used to study the output asymmetry by introducing power-dependent losses near one facet. It was argued that these might be due to a lateral shift of the field into a more absorbing region. In another type of longitudinal model, the lateral dimension is included, but the assumption is made that the field consists of a local normal mode, which is transferred adiabatically through the structure. This assumption only holds if the non-linearity, due to stimulated emission, is sufficiently weak. In both the purely longitudinal and the local normal mode approach, the method implies that the mode gain at a given position  $z$  is identical for forward and backward traveling field.

A full longitudinal-lateral model has been reported in [13]–[15]. In all cases the beam propagation method (BPM) is used to propagate the field back and forth through the  $z$ -dependent structure. In [16] this method was used to compare a longitudinal model with a purely lateral model on one specific laser with facet reflectivities of 32 percent. The conclusion was that the differences in output power for a given current were minor.

In this paper such a comparison is pursued for low reflectivity lasers. It will be shown that the differences become

Manuscript received September 24, 1984; revised November 26, 1984. This work was supported in part by the Belgian National Fund for Scientific Research (NFWO).

The authors are with the Laboratory for Electromagnetism and Acoustics, University of Gent, St. Pietersnieuwstraat 41, B-9000, Gent, Belgium.

more pronounced. Moreover, the longitudinal model is able to predict power asymmetries in the two output beams without introducing any explicit  $z$ -dependencies in the laser geometry.

In the next section the calculation method will be explained in some detail and the assumptions built in the model will be stated. Next, in Section III the model will be applied to two quite different gain-guided lasers and conclusions will be made.

## II. THE CALCULATION METHOD

In our method we also make use of a number of assumptions and simplifications. First, an imposed form is used for the lateral current spreading [7] and longitudinal variations are not included. This means that the current injection is in fact not consistent with the carrier concentration, which itself is derived from a diffusion equation with an effective diffusion constant [17]. This diffusion constant and also the spontaneous recombination time is assumed to be constant, although this is not a basic limitation to the method. The time dependent term is left out because only static solutions are considered. The carrier diffusion in longitudinal direction is neglected because the source term varies either rapidly (i.e., the standing wave pattern caused by interference of forward and backward traveling waves) or very slowly with respect to the diffusion length.

The gain and refractive index variation are assumed to vary linearly with respect to the carrier density. The effect of temperature on the refractive index is not taken into account explicitly, but a built-in refractive index variation can be included easily.

The wave propagation phenomena are also approximated. First, only one imposed wavelength is considered, which means that neither the laser spectrum, nor the spontaneously emitted light can be calculated. The transversal  $x$ -dimension is eliminated by the effective index method, which implies that the  $x$ -variation of the field has a simple single-mode behavior with one polarization state (TE). At the laser facets, a very simple reflection law is applied: the reflected field is simply proportional to the incident field. This is a quite accurate approximation if the reflection coefficient of the transversal mode is used.

The method does not discriminate between longitudinal modes and the current is limited to values between threshold and onset of a second lateral mode (although multilateral mode operation can be analyzed with the model).

Finally, spontaneous emission is not introduced in the field equations (although it is of course considered in the equation for the carrier density). At or around threshold, the model will therefore not predict the light output accurately, but well above threshold the effect of spontaneous emission on light power is minor in most laser types.

With these assumptions the model is governed by the following equations:

$$J(y) = \begin{cases} J_e & |y| \leq s/2 \\ \frac{J_e}{1 + \frac{|y| - s/2}{l_o}} & |y| \geq s/2 \end{cases}$$

where

$$l_o = \sqrt{\frac{C}{R_y J_e}}, \quad C \approx \frac{4kT}{q} \quad (1)$$

This is the imposed form of the injected current density, as related to the device dimensions.

From the current density, the electron concentration is found by solution of the diffusion equation

$$D_e \frac{d^2 N}{dy^2} + \frac{D_e}{W_a} \frac{dW_a}{dy} \frac{dN}{dy} - \frac{N}{\tau_s} = -\eta \frac{J}{qW_a} + \frac{g\Gamma}{h\nu} (|G_F|^2 + |G_B|^2) \quad (2)$$

which is derived from charge continuity considerations.

The gain and refractive index vary linearly with the electron density.

$$g(y, z) = AN(y, z) - B \quad [\text{as used in (2)}] \quad (3)$$

$$g'(y, z) = g(y, z) - (A'N(y, z) + B') \quad [\text{as used in (8)}] \quad (4)$$

$$\Delta n_r(y, z) = -C \cdot N(y, z). \quad (5)$$

Finally, the field propagation is described by the effective index approximation and the simple reflection law as follows:

$$E_y(x, y, z) = F(x, y) \cdot G(y, z) \quad (6)$$

$$\nabla_{yz}^2 G + k_o^2 n_{\text{eff}}^2 G = 0 \quad (7)$$

$$n_{\text{eff}}^2 = n_{\text{eff},0}^2 + 2\Delta n_{\text{bi}}(n_a \Gamma + n_p(1 - \Gamma)) + 2 \left( \Delta n_r + \frac{ig'}{2k_o} \right) n_a \Gamma \quad (8)$$

$$G_B(y, z=L) = \sqrt{R_2} G_F(y, z=L) \quad (9)$$

$$G_F(y, z=0) = \sqrt{R_1} G_B(y, z=0). \quad (10)$$

The meaning of the various symbols in these equations is as follows:

- $J(y)$  = current density
- $N(y, z)$  = carrier density
- $g(y, z)$  = gain distribution
- $\Delta n_r(y, z)$  = refractive index variation (real part)
- $\Delta n_{\text{bi}}(y, z)$  = built-in index variation (real)
- $E_y(y, z)$  =  $y$ -component of the electric field
- $F(x, y)$  = transversal field distribution
- $G(y, z)$  = lateral and longitudinal field distribution
- $n_{\text{eff}}(y, z)$  = effective refractive index
- $s$  = stripewidth
- $R_y$  = spreading resistance
- $W_a$  = active region thickness
- $D_e$  = effective diffusion constant
- $\tau_s$  = spontaneous recombination time
- $\eta$  = efficiency factor for current injection
- $\Gamma$  = field filling factor
- $n_a$  = unperturbed active layer refractive index (complex)

$n_p$  = unperturbed passive layer refractive index (complex)

$n_{eff,0}$  = effective refractive index of unperturbed double heterostructure slab

$A, B, C$ : coefficients for gain and index variation

$R_1, R_2$ : power reflectivities for the TE-mode  $F$  at facet 1 and 2.

Due to the interaction between the electromagnetic field and the dielectric structure, any solution method for this set of equations is necessarily iterative. In our method this iteration consists of the propagation of a trial field back and forth through the laser structure, with simultaneous solution of the diffusion equation, until a stable field pattern is found for the whole cavity.

The stimulated emission term in the diffusion equation is calculated by adding the backward propagating field of the previous iteration cycle to the current forward propagating field, and vice versa.

For the field propagation, we make use of the beam propagation method (BPM) [18]. This method consists of a stepwise solution of a Helmholtz equation, starting from a given field distribution at one boundary. The validity of this method is guaranteed if the refractive index variation is sufficiently slow and small, if the propagation is paraxial, and if distributed reflections can be neglected [19]. The diffusion equation is solved by a straightforward finite difference method. Convergence is mostly obtained after 5–20 propagation round-trips. It is evident that this convergence speed depends strongly on the initial trial field. Therefore, we normally start by doing a nonlongitudinal calculation and use its solution as the start field. This nonlongitudinal calculation can easily be done by the same method, by spreading the mirror losses over the cavity.

The uniqueness of the solution is not always guaranteed, as will be shown in the Section III. In a number of cases several solutions were found, both in the nonlongitudinal analysis and in the longitudinal analysis. These different solutions cannot coexist however, due to the nonlinearity of the problem. Both stable and unstable solutions can be found. An unstable solution will disappear as soon as a small perturbation is introduced in an adequately chosen laser parameter. When several stable solutions exist, the choice of the initial field distribution, or the numerical noise will determine which solution is obtained finally. In an actual laser, small geometrical deviations or nonuniformities will probably favor one solution over the others.

### III. CALCULATION EXAMPLES

In this section the calculation of the two different lasers will be presented and discussed. Table I shows the parameters of the two lasers. The first laser is the same as the one considered in [4], except for the facet reflectivities which are chosen to be 1 percent here instead of 32 percent. A comparison between the longitudinal and nonlongitudinal analysis for  $R_1 = R_2 = 32$  percent has already been reported in [16]. The conclusion was that the differences were minor at current levels

TABLE I

parameter	laser1	laser2
$s$ ( $\mu\text{m}$ )	12.	5.
$L$ ( $\mu\text{m}$ )	300.	500.
$w_a$ ( $\mu\text{m}$ )	0.2	0.4
$R_1, R_2$	0.01	0.01
$\lambda$ ( $\mu\text{m}$ )	0.9	0.9
$n_a$	$3.6-71.6 \cdot 10^{-6}j$	$3.6-71.6 \cdot 10^{-6}j$
$n_p$	$3.4-0.215_8 \cdot 10^{-3}j$	$3.4-0.215_8 \cdot 10^{-3}j$
$A$ ( $\mu\text{m}^{-2}$ )	$3.0 \cdot 10^{-8}$	$6.0 \cdot 10^{-8}$
$B$ ( $\mu\text{m}^{-1}$ )	$4.0 \cdot 10^{-2}$	$8.0 \cdot 10^{-2}$
$A'$ ( $\mu\text{m}^{-1}$ )	$1.0 \cdot 10^{-9}$	0.
$B'$ ( $\mu\text{m}^{-3}$ )	$1.15 \cdot 10^{-3}$	0.
$C$ ( $\mu\text{m}^{-3}$ )	$-5.0 \cdot 10^{-9}$	$-17.19 \cdot 10^{-9}$
$D_e$ ( $\mu\text{m}^2/\text{ns}$ )	3.6	2.0
$\tau_{sp}$ (ns)	2.5	2.
$R_y$	=	=
$\eta$	1.	1.
$\Delta n_{bi}$	yes	no

$$\Delta n_{bi} = \begin{cases} \Delta n_{max} \cdot (1 - ((y-\delta) / (3s/4))^2) & \text{when } |y-\delta| < 3s/4 \\ 0. & \text{when } |y-\delta| > 3s/4 \end{cases}$$

Where  $\Delta n_{max} = 0.003$  and  $\delta = 0.1 \mu\text{m}$ .

below the onset of a second mode. The threshold current  $I_{th}$  of this laser was 104.5 mA and the light-current characteristic is shown in Fig. 1(a). The strong deviation from linearity for currents beyond 135 mA is due to a lateral shift of the intensity distribution away from the gain peak, which shifts in the opposite direction. Such an effect is typical for a broad stripe laser. A lateral symmetric solution still exists at these current levels, but it is unstable at the smallest perturbations and will disappear in favor of one of the lateral asymmetric solutions. The almost negligible differences between the longitudinal and nonlongitudinal models are due to the relatively small variations in total power of about 17 percent over the length of the cavity.

For  $R_1 = R_2 = 1$  percent the situation is different. In this case, the ratio of maximum to minimum power over the length of the cavity is about 5, and a gain saturation effect can be expected. This means that the growth in power of the forward or backward propagating field does not behave exponentially anymore. Fig. 1(a) illustrates the light-current characteristic calculated with both the nonlongitudinal (dashed line) and the longitudinal (full line) model. The threshold current was 143.5 mA in this case and it can be seen that the differential quantum efficiency as well as the maximal power output of the onset of a second lateral mode are higher than for  $R_1 = R_2 = 32$  percent. As expected, there is a larger discrepancy in the output power between the two methods, up to about 6.5 percent. Internally in the laser the differences are even larger. This is shown in Fig. 1(b), which depicts the power of the traveling waves along  $z$ . The dashed line shows a purely exponential increase as derived from the nonlongitudinal calculation. The figure shows that the gain is smaller at the facet, as a consequence of a smaller electron concentration, related to a higher power. This can also be seen in Fig. 1(c). The carrier density is not only smaller at the facet, but the profile itself differs from that at the center due to increased spatial hole burning.

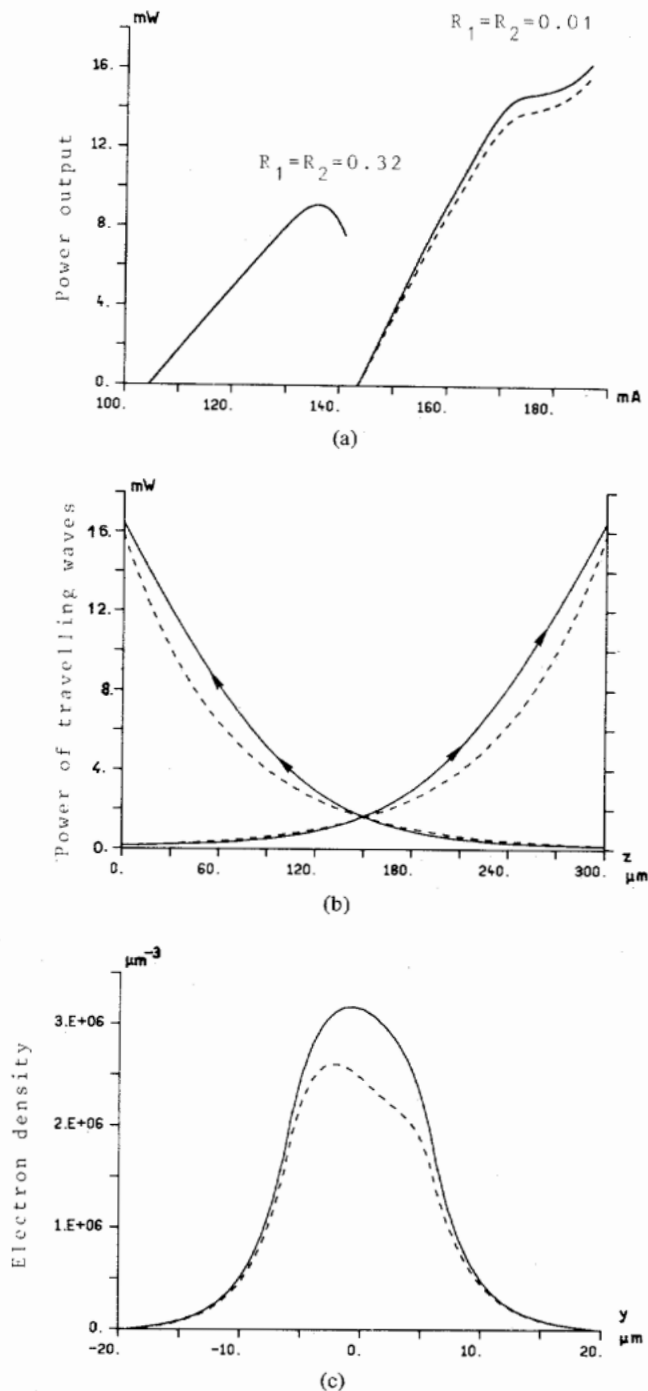


Fig. 1. (a) Light-current characteristic for the first laser, (nonlongitudinal model in dashed line). (b) Total propagating power as a function of  $z$  (exponential increase in dashed line). (c) Electron density as a function of  $y$  at facet (full line) and in the middle (dashed line).

The field profile at the facet differs slightly from the laser center, being about  $1 \mu\text{m}$  wider at its 3 dB-points.

The parameters of the second laser have been chosen rather arbitrarily. The facet reflectivities are again 1 percent. The gain and antiguiding parameters have been chosen relatively strong, so the longitudinal effects can be expected to become more important. Because these parameters are not meant to be realistic, the results are only of qualitative value, i.e., they overemphasize certain effects. A built-in refractive index was

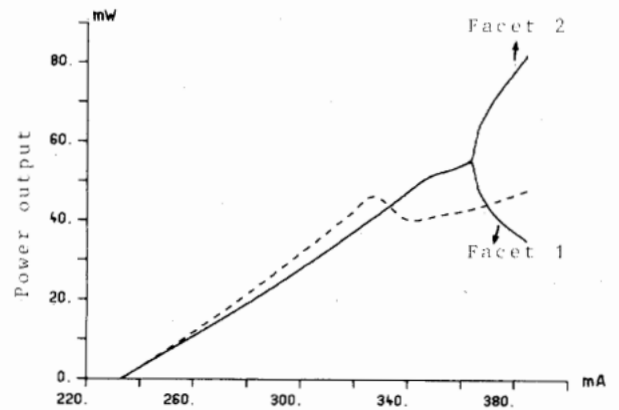


Fig. 2. Light-current characteristic for the second laser, for both facets 1) and 2), (nonlongitudinal model in dashed line).

not included. Fig. 2 shows the light-current curve up to onset of a second mode for both mirrors as obtained by the longitudinal method, as well as the nonlongitudinal characteristic (dashed line). The two methods give a quite big difference now. Moreover, we observe an asymmetrical light output at currents above  $1.57 I_{th}$ . The threshold current of this laser is about 233 mA (high due to the thick active layer of  $0.4 \mu\text{m}$ ). At or around threshold the differences between the two methods are minor because of the negligible impact of the field power on the electron density.

The asymmetric output is a very remarkable phenomenon. It is generally considered as an undesirable property. To our knowledge, this is the first report of a combined longitudinal-lateral model which predicts different outputs from both facets, in nominally symmetric (in  $z$ -direction) lasers. In [12] a lot of possible reasons for producing an asymmetric output have been ruled out by careful examination, and the appearance of such an asymmetry could only be modeled by introducing extra power-dependent losses near one facet. As the gain is identical for both forward and backward propagating fields in that model, the spontaneous emission is essential to obtain asymmetric outputs. The coupling efficiency of the spontaneous emission was chosen such that the calculated results fitted experimental data. In our model the field intensity profile of forward and backward propagating waves is allowed to be different. In this way the power gain (as integrated over  $y$ ) will be different for these two waves. This situation is sometimes called anisotropy in the gain (although it has nothing to do with material anisotropy). In [12] such an anisotropy is considered unlikely, but our model shows an example that it may happen. This gain anisotropy has a direct influence on the output symmetry of the laser, and even without introducing spontaneous emission different outputs from the two facets (with equal mirror reflectivity) can be found. The ratio of the two output powers is in general given by

$$\frac{P_{out,2}}{P_{out,1}} = \frac{1 - R_2}{1 - R_1} \cdot \sqrt{\frac{R_1}{R_2}} \cdot \exp \frac{1}{2} \int (g_{P,F}(z) - g_{P,B}(z)) dz \quad (11)$$

where  $g_{P,F}(z)$  and  $g_{P,B}(z)$  are the power gains of the forward and backward traveling fields respectively.

At first sight, it might seem surprising that a longitudinally symmetric structure produces asymmetric light outputs. However, the structure seen by the optical fields (i.e., refractive index profile) is not longitudinally symmetric anymore as soon as the field is asymmetric itself, because of the influence of the field on the refractive index through simulated emission.

In Fig. 3-5 a number of calculation data are drawn for one particular value of the current, i.e., 60 percent above threshold. Fig. 3(a) shows the total power as a function of  $z$  for the traveling waves. It can be observed that for the backward traveling wave the power decreases before it increases, whereas the forward traveling beam tends to saturate near the facet. This is even more clearly shown in Fig. 3(b) where the power gain is drawn. In order to obtain different gains at a given position  $z$ , the forward and backward traveling waves need to have a different field distribution. This is illustrated in Fig. 3(c), which shows the position (in the lateral  $y$ -direction) of the maximal intensity and of the 3 dB-points of the intensity distribution as a function of  $z$ , for both waves. Near the high output mirror, the backward traveling wave moves towards negative  $y$ -values and broadens a great deal. This causes the power gain to become negative near that facet. According to (11), this results in an asymmetrical output power. The fact that backward and forward propagating waves have a different behavior near the high output facet is mainly due to the fact that the impact of the fields on the carrier concentration is dominated by the strong forward propagating field. In other words, this field has a larger inertia for shifting away due to the reaction capacity of the refractive index. In Fig. 4 the carrier density is shown at the two facets and also at the position of minimum total power. The latter shows only little spatial hole burning, whereas a strong influence of the fields is evident at the facets. The relatively strong electron density at facet 2 between  $y = -15 \mu\text{m}$  and  $y = -5 \mu\text{m}$  is due to absorption of the optical power in that region. Fig. 5(a) and (b) depict the normalized near- and far-field intensities, respectively, at both facets. The dashed line in shows the nonlongitudinal solution. In [20] a theoretical model has been proposed to explain the often observed asymmetry between both facets in far-field distributions. The power asymmetry between both facets increases rapidly with increasing current and the position of minimal total power shifts further towards one of the facets.

One may wonder whether there are other field solutions for this laser. Since the nominal structure is symmetric, it is evident that an asymmetric solution will have two versions, which are each other's image. Since the solution presented in Figs. 3-5 is asymmetric both in the  $y$ -direction and the  $z$ -direction, there are at least four solutions. We have investigated the existence of a (longitudinally) symmetric solution. Therefore, we have put a mirror of 100 percent reflectivity in the middle of the cavity and have looked for a solution in this half cavity at a current of  $0.8 I_{th}$  (corresponding to  $1.6 I_{th}$  for the full laser). Every solution of this is also a solution to the full laser, with longitudinal symmetry. Such a solution could indeed be found and Fig. 6(a)-(c) shows the power, the power gain, and also the position of maximum and half power density as a function of  $z$ , for both traveling waves. Again this solution is not symmetric in lateral direction, which means that there are two

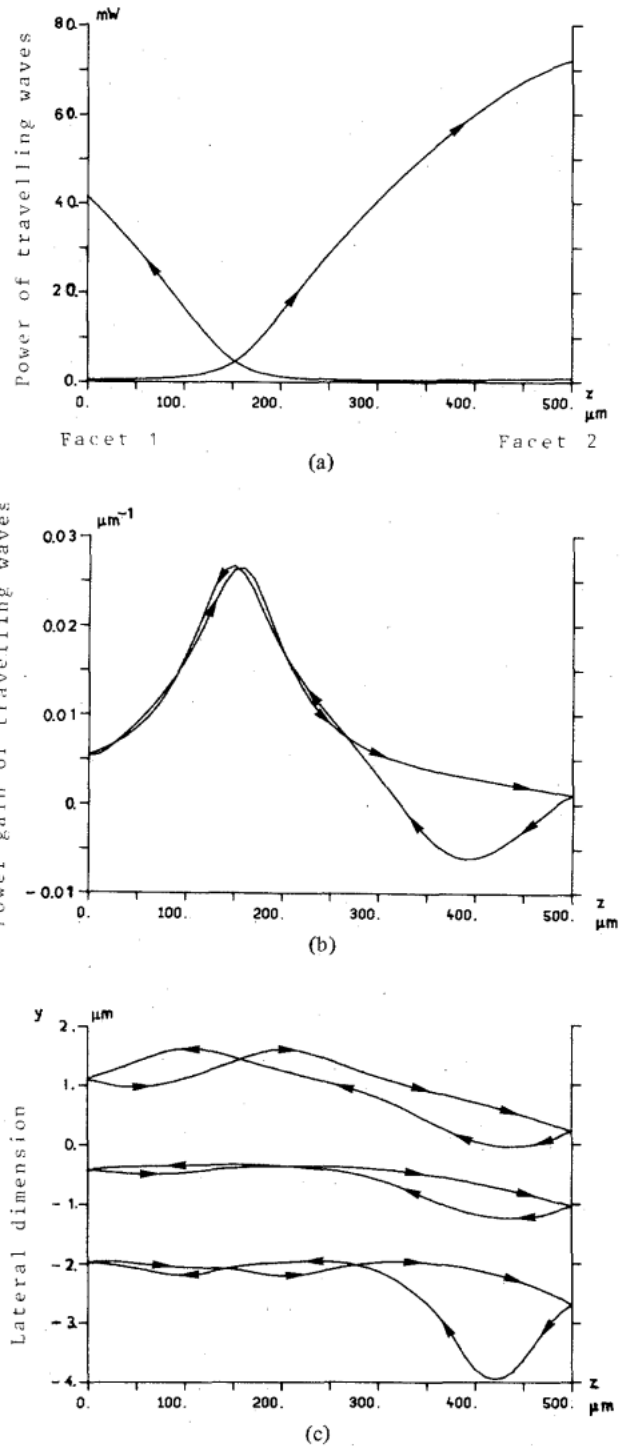


Fig. 3. Total power as a function of  $z$  for the traveling waves in laser 2 at  $1.6 I_{th}$ . (b) Total power gain as a function of  $z$ , for both traveling waves in laser 2. (c) Lateral position of the maximal intensity and of the two 3 dB-points of the intensity distribution.

such solutions. This longitudinally symmetric field solution was now introduced in the model for the full laser and was shown to be a solution indeed. However, the numerical noise was already sufficient for this solution to disappear in favor of one of the longitudinally asymmetric solutions described earlier. It could of course not be predicted too which one of the longitudinal asymmetric solutions the symmetric solution

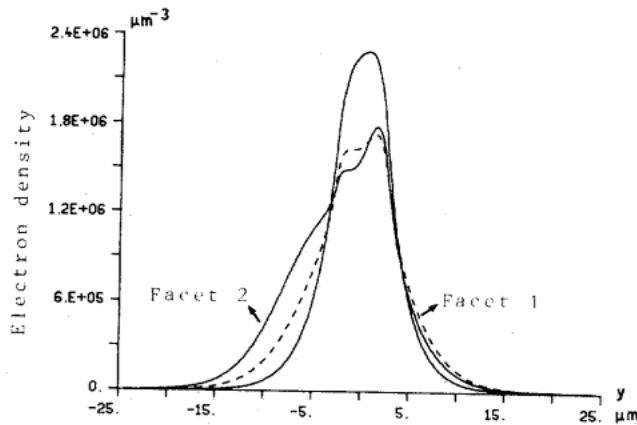


Fig. 4. Carrier density at both facets 1) and 2) and at the position of minimal total power.

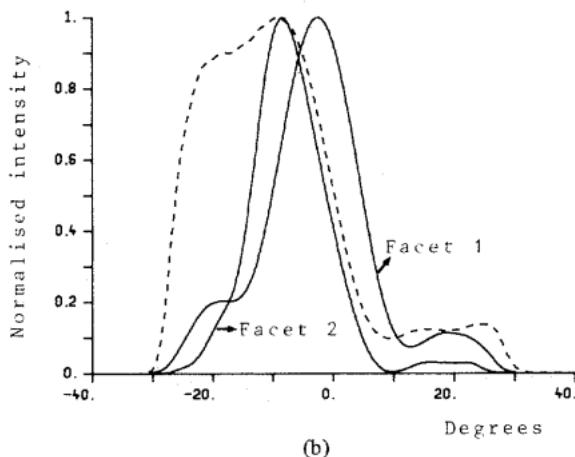
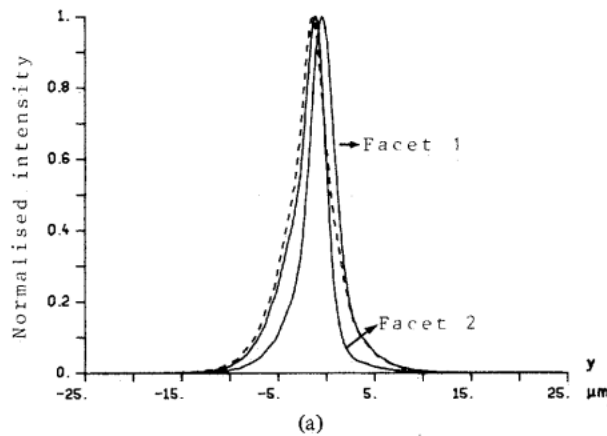


Fig. 5. (a) Near fields at both facet 1) and 2) (nonlongitudinal model in dashed line). (b) Far fields at both facet 1) and 2) (nonlongitudinal model in dashed line).

would evolve. Unlike many cases where 5-10 propagation roundtrips are sufficient for convergence, many more were needed in this particular case, because the shift away from the symmetric solution is very slow. From this it was concluded that the symmetric solution is unstable and will not be met in a real laser.

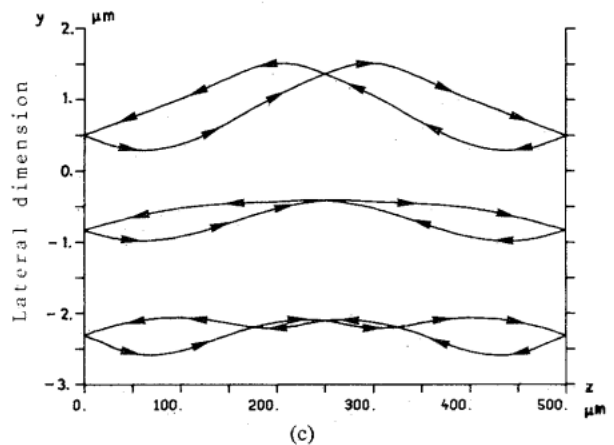
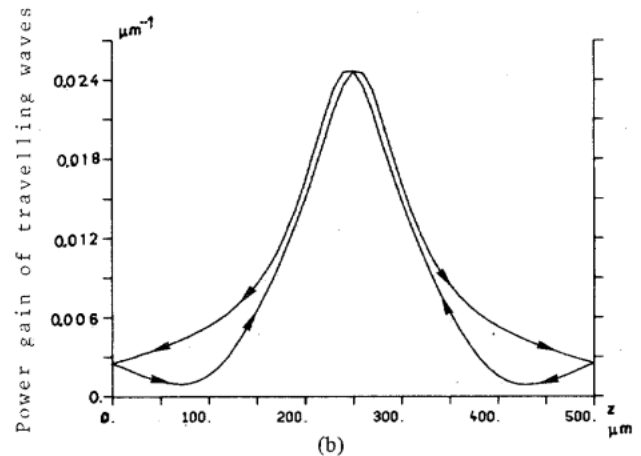
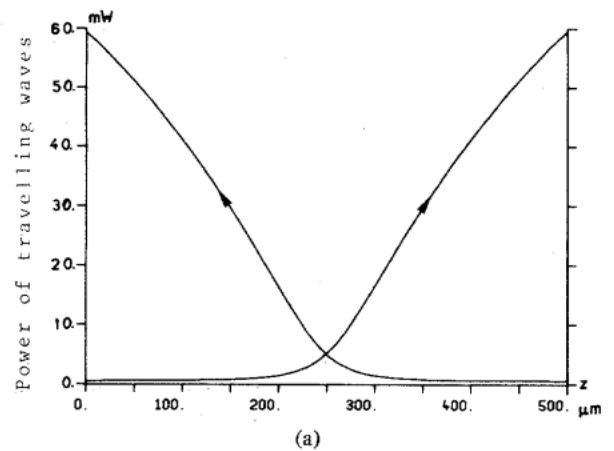


Fig. 6. (a) Total power as a function of  $z$  in laser 2, for the (unstable) symmetric solution. (b) Lateral position of the maximal intensity and of the two 3 dB-points of the intensity distribution for the symmetric solution, (b) Total power gain as a function of  $z$ , for the symmetric solution, for both traveling waves in laser 2.

It is observed experimentally that power asymmetries do occur more in lasers fabricated by LPE than those fabricated by MOVPE or MBE [12]. This suggests that these asymmetries are related to growth defects or layer nonuniformities. In this paper a longitudinal asymmetry was found theoretically even for a perfect laser. This is not necessarily in contradiction to the experimental observations, because a nonuniformity may

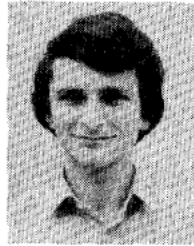
well cause the symmetry breakdown to occur at lower power values than in the equivalent perfect laser. This is under further investigation now.

#### IV. CONCLUSION

A combined lateral-longitudinal model has been described and applied to two perpendicular lasers with low reflectivity facets. It was shown that the resulting solution for the output fields may differ significantly from that of a purely lateral model. However, longitudinally asymmetric field solutions were found in a nominally symmetric laser. These were shown to be due to a difference in the power gain for the traveling fields caused by field distributions which are different for forward and backward propagating waves. These phenomena may be related to the experimentally observed output asymmetries in some semiconductor lasers.

#### REFERENCES

- [1] J. Buus, "Principles of semiconductor laser modeling," *IEE Proc.*, part J, vol. 132, no. 1, pp. 42-51, 1985.
- [2] P. M. Asbeck, D. A. Cammack, J. Daniele, and V. Klebanoff, "Lateral mode behavior in narrow stripe lasers," *IEEE J. Quantum Electron.*, vol. QE-15, pp. 727-733, 1979.
- [3] W. Streifer, R. D. Burnham, and D. R. Scifres, "Channeled substrate nonplanar laser analysis—Part I: Formulation and the plano-convex waveguide laser," *IEEE J. Quantum Electron.*, vol. QE-17, pp. 736-744, 1981.
- [4] J. Buus, "Models of the static and dynamic behavior of stripe geometry lasers," *IEEE J. Quantum Electron.*, vol. 953-960, 1983.
- [5] —, "The effective index method and its applications to semiconductor lasers," *IEEE J. Quantum Electron.*, vol. QE-18, pp. 1083-1089, 1982.
- [6] W. Streifer and E. Kapon, "Application of the equivalent index method to DH diode lasers," *Appl. Opt.*, vol. 18, pp. 3724-3725, 1979.
- [7] H. Yonezu, I. Sabuma, K. Kobayashi, T. Kamejina, M. Ueno, and Y. Nannichi, "A GaAs-AlGaAs double heterostructure planar laser," *Japan. J. Appl. Phys.*, vol. 12, pp. 1585-1592, 1973.
- [8] D. P. Wilt and A. Yariv, "A self-consistent static model of the double heterostructure laser," *IEEE J. Quantum Electron.*, vol. QE-17, pp. 1941-1949, 1981.
- [9] D. R. Scifres, W. Streifer, and R. D. Burnham, "Curved stripe GaAs:GaAlAs diode lasers and waveguides," *Appl. Phys. Lett.*, vol. 32, pp. 231-234, 1978.
- [10] D. Fekete, W. Streifer, D. R. Scifres, and R. D. Burnham, "High speed laser modulation with integrated optical injection," *Appl. Phys. Lett.*, vol. 37, pp. 975-978, 1980.
- [11] J. E. A. Whiteaway and G. H. B. Thompson, "Optimisation of power efficiency of (GaAl)As injection lasers operating at high power levels," *Solid State, Electron. Dev.*, vol. 1, pp. 81-88, 1977.
- [12] D. Marcuse and F. R. Nash, "Computer model of an injection laser with asymmetrical gain distribution," *IEEE J. Quantum Electron.*, vol. QE-18, pp. 30-43, 1982.
- [13] G. P. Agrawal, W. B. Joyce, R. W. Dixon, and M. Lax, "Beam propagation analysis of stripe-geometry semiconductor lasers: Threshold behaviour," *Appl. Phys. Lett.*, vol. 43, 1983.
- [14] R. Baets and P. E. Lagasse, "Longitudinal static-field model for DH lasers," *Electron. Lett.*, vol. 20, pp. 41-42, 1984.
- [15] P. Meissner, E. Patzak, and D. Yevick, "A self-consistent model of stripe geometry lasers: Based on the beam propagation method," *IEEE J. Quantum Electron.*, vol. QE-20, pp. 899-905, 1984.
- [16] R. Baets and J. Buus, "Comparison of a beam propagation model for laser diodes with other modeling techniques," to be published.
- [17] W. B. Joyce, "Carrier transport in double-heterostructure active layers," *J. Appl. Phys.*, vol. 53, pp. 7235-7239, 1982.
- [18] P. E. Lagasse and R. Baets, "The beam propagation method in integrated optics," to be published.
- [19] J. Van Roey, J. van der Donk, and P. E. Lagasse, "Beam-propagation method: Analysis and assessment," *J. Opt. Soc. Amer.*, vol. 71, pp. 803-810, 1981.
- [20] J. E. Kardontchik, "Far field asymmetry in narrow stripe gain-guided lasers," *IEEE J. Quantum Electron.*, vol. QE-18, pp. 1287-1294, 1982.



Roel Baets received the degree in electrical engineering from the University of Ghent, Ghent, Belgium, in 1980. He received the M.Sc. degree from Stanford University, Stanford, CA, and the Ph.D. degree from the University of Ghent in 1980 and 1984, respectively.

He is now with the Interuniversity Microelectronics Center (IMEC), working in the III-V group at the university of Ghent. His current interests include epitaxial growth of III-V compounds, optoelectronic integrated circuits, and modeling of semiconductor lasers.



Jean-Pierre Van de Capelle was born in Ghent, Belgium, on March 12, 1961. He received the degree in electrical engineering from the University of Ghent in 1984.

He is currently working toward the Ph.D. degree at the University of Ghent.



P. E. Lagasse (M'83) received the degree in electrical engineering in 1969 and the Ph.D. degree in 1972, both from the University of Ghent, Ghent, Belgium.

In 1981 he became Professor of Electrical Engineering at the University of Ghent. He has been working in the fields of SAW, optoelectronics, and high frequency technology.

Prof. Lagasse is a member of the optical Society of America, and the Acoustical Society of America.